



Published in final edited form as:

*Mol Pharm.* 2007 ; 4(2): 289–297. doi:10.1021/mp060117f.

## A New Method for Delivering a Hydrophobic Drug for Photodynamic Therapy Using Pure Nanocrystal Form of the Drug

Koichi Baba<sup>1</sup>, Haridas E. Pudavar<sup>1</sup>, Indrajit Roy<sup>1</sup>, Tymish Y. Ohulchanskyy<sup>1</sup>, Yihui Chen<sup>2</sup>, Ravindra Pandey<sup>2</sup>, and Paras N. Prasad<sup>1</sup>

<sup>1</sup> Institute for Lasers, Photonics and Biophotonics, SUNY at Buffalo, Buffalo, New York 14260

<sup>2</sup> Photodynamic Therapy Center, Roswell Park Cancer Institute, Buffalo, New York 14263

### Abstract

A carrier free method for delivery of a hydrophobic drug in its pure form, using nanocrystals (nano sized crystals) is proposed. To demonstrate this technique, nanocrystals of a hydrophobic photosensitizing anticancer drug 2-devinyl-2-(1-hexyloxyethyl)pyropheophorbide (HPPH), have been synthesized using re-precipitation method. The resulting drug nanocrystals were monodispersed and stable in aqueous dispersion, without the necessity of an additional stabilizer (surfactant). As shown by confocal microscopy, these pure drug nanocrystals were taken-up by the cancer cells with high avidity. Though the fluorescence and photodynamic activity of the drug were substantially quenched in the form of nanocrystals in aqueous suspension, both these characteristics were recovered under in vitro and in vivo conditions. This recovery of drug activity and fluorescence is possibly due to the interaction of nanocrystals with serum albumin, resulting in conversion of the drug nanocrystals into the molecular form. This was confirmed by demonstrating similar recovery in presence of Fetal Bovine Serum (FBS) or Bovine Serum Albumin (BSA). Under similar treatment conditions, the HPPH in nanocrystal form or in 1% Tween 80/water formulation showed comparable in vitro and in vivo efficacy.

### Keywords

nanocrystals; re-precipitation method; photosensitizers; photodynamic therapy; singlet oxygen; drug delivery

### Introduction

Many of the commonly used pharmaceutical agents including various drugs are hydrophobic in nature. Therefore for delivery of these drugs, special formulations are required to make their aqueous dispersion, using surfactants or other nanoparticle based delivery vehicles. Upon systemic administration, such drug-doped carriers are preferentially taken up by tumor tissues by the virtue of the 'Enhanced Permeability and Retention Effect',<sup>1-7</sup> which is the property of such tissues to engulf and retain circulating macromolecules and particles owing to their 'leaky' vasculature. The carriers include oil-dispersions (micelles), liposomes, polymeric micelles, hydrophilic drug-polymer complexes, ceramic and polymeric nanoparticles, etc.<sup>8-14</sup> However many surfactants themselves, or in some cases the byproducts produced during preparation of these surfactant based drug dispersions, tend to increase the systemic toxicity of the drug formulation. Therefore, there is increasing interest in the development of novel drug

formulation and delivery methods, without the addition of any external agents such as surfactants or other carrier vehicles. One method proposed for dispersion of hydrophobic compound in water is the “Reprecipitation method”.<sup>15-17</sup> Though the nanocrystal formation of hydrophobic compounds has been well studied,<sup>18, 19</sup> there has been no report of using this technique for drug delivery. To demonstrate this concept, we have prepared the nanocrystal formulation of a hydrophobic drug for photodynamic therapy and compared its efficacy with the conventional surfactant-based formulation.

Photodynamic therapy (PDT) is a promising new modality for the treatment of a variety of cancers as well as some dermatological and ophthalmic diseases<sup>1, 20-24</sup> The main advantage of PDT over conventional cancer chemotherapy is the capability to localize the treatment, by using selective light exposure to the tumor site.<sup>1, 25</sup> Typical PDT treatment involves systemic administration of a photosensitizer drug, followed by localized light exposure at the tumor site, using visible or near-infrared (NIR) light. After being excited with light, these photosensitizer molecules can transfer their excited state energy to molecular oxygen in the surrounding, forming reactive oxygen species (ROS) such as singlet oxygen ( $^1O_2$ ). These locally generated ROS are responsible for the destruction of various cellular compartments resulting in irreversible damage of tumor cells.<sup>1, 25-30</sup> Since this destruction process requires a combination of three essential components (photosensitizer, light and oxygen), PDT can be used to selectively destroy diseased tissues such as tumors, with relatively minimal collateral damage.<sup>25</sup>

The major drawback for successful pre-clinical and clinical PDT is the poor water solubility of photosensitizing (PS) drugs, which makes their stable formulation for systemic administration highly challenging.<sup>1, 31</sup> To overcome this difficulty, different strategies have evolved to enable a stable dispersion of these drugs into aqueous systems, often by means of a delivery vehicle.<sup>32</sup> These delivery vehicles often unfavorably affect the inherent tumor-avid pharmacokinetics of the PS drugs, resulting in the possibility of sub-therapeutic dosage at the tumor site. Also, allergic reactions emanating from the carrier vehicles as well as their sustained *in vivo* persistence results in short as well as long-term toxicities, which may override the successful outcome of PDT.<sup>3, 4</sup> Therefore, the ideal formulation for safe and efficient PDT should involve the minimal number of additional ingredients apart from the PS drug.

Here we report a new method for the delivery of water insoluble PS drugs without the incorporation of any additional stabilizing agents such as surfactants or other delivery vehicles. This new drug formulation method is based on the re-precipitation method,<sup>15-17</sup> whereby upon injection of the drug dissolved in a miscible solvent like DMSO into water, the drug molecules self-assemble as pure nanosized crystals and remain stably dispersed in water. For demonstrating this method, we have synthesized nanocrystals of the PS 2-devinyl-2-(1-hexyloxyethyl) pyropheophorbide (HPPH) by re-precipitation method. HPPH is an effective PS which is in Phase I/II clinical trials at Roswell Park Cancer Institute, Buffalo, NY, USA.<sup>33-38</sup> The resulting nanocrystals are monodispersed, with diameter ~100 nm. Though the fluorescence and photodynamic activity of the drug nanocrystals were substantially quenched in aqueous media, both recovered under *in vitro* and *in vivo* conditions. The recovery of fluorescence and photodynamic activity inside cells were verified by confocal microscopy and cellular phototoxicity assay. This recovery of drug activity and fluorescence is attributed to the interaction of nanocrystals with blood serum or other intracellular components (e.g., serum albumin), resulting in conversion of the drug nanocrystals into the molecular form. This was confirmed by showing a similar recovery in the presence of Fetal Bovine Serum (FBS) or Bovine Serum Albumin (BSA). Efficacy of the nanocrystal formulation *in vitro* as well as *in vivo* was found to be comparable with that of the same drug formulated in the conventional delivery vehicle, Tween-80.

## Experimental Section

**Materials**—Surfactant Tween-80 was purchased from Aldrich, USA. MTT [3-(4,5-dimethylthiazol-2-yl)-2,5-diphenyltetrazolium bromide], Bovine Serum Albumin (BSA) and are products of Sigma, USA. Dimethyl Sulfoxide (DMSO) and isopropanol are products of Fisher Chemicals, USA. The photosensitizer, 2-[1-hexyloxyethyl]-2-devinyl pyropheophorbide-a (HPPH), was prepared by following the methodology reported by Pandey et al. Cell culture products, unless mentioned otherwise, were purchased from GIBCO. The RIF-1 cell line was obtained from the PDT Center, Roswell Park Cancer Institute, Buffalo. Cells were cultured according to instructions supplied by the vendor. N,N-dimethyl formamide (DMF) was purchased from Fisher Chemicals, USA. Cell culture products, unless mentioned otherwise, were purchased from GIBCO, USA. All the above chemicals were used without any further purification.

**Synthesis and Characterization of Drug Nanocrystals**—Re-precipitation method for the preparation of nanocrystals of hydrophobic dyes as well as the crystalline structure of the resulting nanoparticles had been extensively studied by the Nakanishi group.<sup>18, 19, 39, 40</sup> A similar approach was used in this case to prepare organic nanocrystals of the hydrophobic PDT drug, HPPH. For this, 200 $\mu$ l of 3mM HPPH solution in DMSO was injected into 10ml of water at room temperature, with controlled stirring. The samples were dialyzed overnight to remove DMSO. Transmission electron microscopy (TEM) was employed to determine the morphology and size of the aqueous dispersion of nanocrystals, using a JEOL JEM 2020 electron microscope, operating at an accelerating voltage of 200 kV. Dynamic light scattering (Brookhaven 90PLUS with ZetaPALS option) was used to determine the size distribution as well as the zeta potential of the nanocrystals. Electron diffraction and X-ray diffraction techniques were used to confirm the crystalline nature of the prepared nanocrystals.

**Optical spectroscopy**—UV-visible absorption spectra were acquired using a Shimadzu UV-3101 PC spectrophotometer, in a quartz cuvette with 1 cm path length. Fluorescence spectra were recorded on a Shimadzu RF-5301PC spectrofluorimeter. Generation of singlet oxygen ( $^1\text{O}_2$ ) was detected by its phosphorescence emission peaked at 1270 nm.<sup>41-44</sup> Time resolved detection of the  $^1\text{O}_2$  emission<sup>45</sup> was used to distinguish singlet oxygen emission, which is known to have extremely low yield in water.<sup>46</sup> A SPEX 270M Spectrometer (Jobin Yvon) equipped with a Hamamatsu IR-PMT coupled to Infinium oscilloscope (Hewlett-Packard) was used for recording singlet oxygen phosphorescence decay. The monochromator was tuned to 1270 nm. The second harmonic (532 nm) from a nanosecond pulsed Nd:YAG laser (Lotis TII, Belarus) operating at 20 Hz was used as the excitation source. The sample solution in a quartz cuvette was placed directly in front of the entrance slit of the spectrometer and the emission signal was collected at 90-degrees relative to the exciting laser beam. An additional longpass filters (a 950LP filter and a 538AELP filter, both from Omega Optical) were used to attenuate the scattered light and fluorescence.

### ***In-Vitro* Studies with Tumor Cells: Nanoparticle Uptake, Imaging and Viability Assay**

**Cell Culture**—The RIF-1 tumor cell line was maintained in alpha-minimum essential medium (R-MEM) with 10% fetal bovine serum (FBS), according to the manufacturers instructions (American Type Culture Collection, Manassas, VA). To study the uptake and imaging of HPPH nanocrystals, the cells were trypsinized and resuspended in the corresponding suitable media at a concentration of around  $7.5 \times 10^5$  /ml. 60  $\mu$ l of this suspension was transferred to each 35 mm culture plate and 2 ml of the corresponding full medium was added. For confocal microscopy, glass bottom petridishes (MatTek corporation) was used in place of standard petri dishes. These plates were then placed in an incubator at 37 °C with 5%  $\text{CO}_2$  (VWR Scientific, model 2400). After 36 hours of incubation, the cells (about 60 % confluency) were rinsed with

PBS, and 2 ml of the corresponding fresh media was added to the plates. Finally, 16.6  $\mu\text{l}$  of 60  $\mu\text{M}$  HPPH nanocrystals suspension (final concentration of 0.5  $\mu\text{M}$  in cell culture media) was added and mixed properly. Plates were returned to the incubator (37 °C, 5 %  $\text{CO}_2$ ) for the required incubation period. 16.6  $\mu\text{l}$  of HPPH/Tween80 micelles of same drug concentration was used as control and separate culture plates were treated and incubated for the same time period as in the case of nanocrystals. After each specific time interval of incubation, the plates were taken out, rinsed several times with sterile PBS and 2 ml of fresh serum free medium was added. The plates were incubated for another 10 minutes at 37 °C and were directly imaged under a confocal microscope.

**Confocal Microscopy**—Confocal imaging was performed using a laser scanning confocal microscope (TCS-SP2-AOBS from Leica), which was attached to an inverted microscope. An oil immersion objective lens (Leica, Fluor-63X, NA 1.4) was used for cell imaging. For confocal imaging, a 405nm diode laser (PicoQuant Germany) was used as the excitation source with spectrally tunable emission filter was set at 650-720 nm. An additional band pass filter (HQ650/100 from Chroma) was also used to cut off any excitation leakage. Cells untreated with the drug were used as control to confirm the absence of any significant autofluorescence under the imaging conditions. We have also obtained intra-cellular spectra under the imaging condition, using the spectral detection available on the Leica Microscope. A comparison of the fluorescence spectra from drug treated cells with the fluorescence spectra of HPPH in solution, allows us to confirm the origin of fluorescence seen in fluorescence image channel.

**In Vitro PDT**—The RIF-1 tumor cells grown in alpha-minimum essential medium ( $\alpha$ -MEM) with 10% fetal calf serum, L-glutamine, and penicillin/streptomycin/neomycin were maintained in 5%  $\text{CO}_2$ , 95% air, and 100% humidity. These cells were plated in 96-well plates at a density of  $5 \times 10^3$  cells/well in complete media, as a means to determine PDT efficacy. The next day, the photosensitizer was added at variable concentrations (0.25 to 8  $\mu\text{M}$ ). After the 24 h incubation in the dark at 37 °C, the cells were replaced with fresh media and exposed to light at a dose rate of 3.2  $\text{mW}/\text{cm}^2$  at various light doses (0.125-8.0 J). The dye laser (375; Spectra Physics, Mt. View, CA) excited by an argon-ion laser (171 laser; Spectra-Physics, Mt. View, CA) was tuned to emit the drug-activating wavelength, 665 nm. Uniform illumination was accomplished using a 600  $\mu\text{m}$  diameter quartz optical fiber fitted with a graded index refraction lens. Following illumination, the plates were incubated at 37 °C in the dark for 48 hours. Appropriate control experiments using identical light doses without any photosensitizer were also performed. After this, the plates were evaluated for cell viability using the MTT assay, as described below.

**Cell Viability Assay**—Cell viability was measured using the 3-[4,5-dimethylthiazol-2-yl]-2,5-diphenyl tetrazoliumbromide (MTT) assay. Immediately following light treatment, the cells were incubated for 44 h in the dark at 37 °C. Then, 10  $\mu\text{L}$  of 4.0 mg/mL solution of MTT dissolved in PBS (Sigma Chemical Co., St. Louis, MO) was added to each well. After the 4 h incubation with the MTT, the media were removed and 100  $\mu\text{l}$  of dimethyl sulfoxide was added to solubilize the formazin crystals. The PDT efficacy was measured by reading the 96-well plate on a microtiter plate reader (Miles Inc., Titertek Multiscan Plus MK II) at an absorbance of 560 nm. The results were plotted as percent survival compared with the corresponding control experiments results (cells were not incubated with drug, but exposed to light). Each data point represents the mean from a typical experiment with four replicate wells.

### Evaluation of *in vivo* Photosensitizing Efficacy

The *in vivo* efficacy of HPPH nanocrystals was compared with HPPH in 1% Tween-80 / water solution under similar treatment conditions.<sup>48</sup> In brief; C3H mice (10 mice/group) were injected subcutaneously in the axilla with  $3 \times 10^5$  RIF-1 cells in 40  $\mu\text{l}$  of complete  $\alpha$ -MEM.

The injected animals developed RIF-1 tumors and the tumors were permitted to grow until they were 4-5 mm in diameter before beginning treatment. The day before PDT light treatment, the mice were injected intravenously with HPPH in 1% Tween-80 / water or HPPH nanocrystals at a dose of 0.4  $\mu\text{mole/kg}$ . Photosensitizers were injected i.v. (tail vein) in approximately 0.2 ml volumes. At 24 h post-injection, mice bearing transplantable tumors were restrained without anesthesia in Plexiglas holders, designed to expose to light only the tumor and a 2-4 mm angular margin of skin. For mice bearing spontaneous tumors at unpredictable sites, light exposure was flexibly adjusted to accommodate exposure of these sites. The mice were treated with a laser light (665 nm, 135 J/cm<sup>2</sup>, 75 mW/cm<sup>2</sup>) for 30 mins.

Following treatment, the tumor dimensions (orthogonal diameters) were measured by caliper every other day for tumor growth/ re-growth assays. The tumor volume,  $V$ , is calculated with the formula  $V=(lw^2/2)$ , where  $l$  is the longest axis of the tumor and  $w$  is the axis perpendicular to  $l$ . Mice were euthanized for ethical consideration when tumors reach the volume of 400 mm<sup>3</sup>. On the other hand, mice were considered cured if there was no palpable tumor by day 60.

## Results and Discussions

HPPH (Photochlor<sup>®</sup>), is a chlorin-based molecule (Fig. 1),<sup>33</sup> which is reported to have an enhanced PDT efficacy than Photofrin<sup>®</sup> (the only photosensitizer currently approved by FDA for clinical PDT).<sup>34, 49</sup> with reduced skin phototoxicity. HPPH is a hydrophobic compound and its long wavelength absorption falls at 665 nm. Therefore, compared to Photofrin<sup>®</sup> ( $\lambda_{\text{max}}$ : 630 nm) it should have deeper tissue penetration. Due to its hydrophobic nature, a conventional formulation of HPPH in water involves the use of surfactants such as Tween-80<sup>34</sup> or the use of other carrier vehicles such as silica –based nanoparticles.<sup>14</sup>

A TEM image of the nanocrystals of the drug HPPH prepared by re-precipitation method is shown in Figure 2A. The particles are nearly spherical, having uniform size distribution, with an average diameter of 110 nanometers. Dynamic light scattering measurements (DLS) also showed reasonably good monodispersity with size ranging from 100-120nm (data not shown). The electron diffraction data obtained from these nanocrystals showed that significant portion of the formed HPPH nanoparticles were crystalline in nature (Figure 2B). X-ray diffraction data also showed crystallinity of the prepared nanocrystals. The average zeta-potential of these nanocrystals were found to be around -40mV. These reasonably high negative surface charges presumably derived from the deprotonation of the carboxylic end groups, provided excellent stability for the water dispersion. The water dispersion of HPPH nanocrystals was found to be stable for more than 3 months.

The UV-visible absorption (Fig.3) as well as the fluorescence emission spectra (Fig.4(A)) of HPPH formulated as nanocrystals are significantly different from those of HPPH dissolved in 1% Tween-80 micelles. This includes suppression of the Soret band and broadening of the long-wave Q-band in the absorption spectra (Fig.3) as well as almost complete quenching of the HPPH emission (Fig. 4 (A)). Similar decrease in fluorescence intensity is well known as aggregation effect for fluorescent molecules<sup>50</sup> and has been reported for chlorins structurally related to HPPH.<sup>47</sup> A decrease in the fluorescence yield in this case correlates with a decrease in the singlet oxygen generation efficiency and is due to the low solubility of the compounds and corresponding aggregation effects.<sup>47</sup>

However, fluorescence of HPPH nanocrystals was found to recover in a time-dependent manner under *in vitro* conditions, in presence of 10% Fetal Bovine Serum (FBS). Typical cell culture media also contain similar concentration of either FBS or Horse Serum. This recovery of fluorescence was attributed to the presence of Bovine Serum Albumin (BSA) and other



lipoproteins in the serum and the drug HPPH seems to have reasonably good solubility in them. Therefore nanocrystals are converted into its molecular form in presence of the serum components, which in turn brings the fluorescence recovery. Serum components of human blood also have similar constituents and we can safely assume that under *in vivo* conditions, similar conversion of the drug nanocrystals can occur. Figure 4 (A) shows the emission spectra of the nanocrystal formulation after 4.5 hrs of incubation with 10% FBS or 0.8% (Wt/Vol) BSA. The time course of the fluorescence recovery in presence of BSA and FBS is shown in figure 4 (B).

Along with fluorescence quenching, the singlet oxygen generation also was initially quenched for this nanocrystal formulation and was found to recover along with the fluorescence emission upon incubation with BSA or FBS. To check the recovery of singlet oxygen generation, we have monitored the decay of spectral signal at 1270 nm, using nanosecond pulsed excitation at 532 nm. Figure 5 shows the decay curves at 1270 nm for HPPH nanocrystals incubated for 24 hrs in MEM $\alpha$  and MEM $\alpha$  with 0.8% BSA. As seen in the figure, the HPPH nanocrystals incubated in MEM $\alpha$  with 0.8% BSA manifest decay in microsecond range, in contrast to nanocrystals in MEM $\alpha$ . Decay in the microsecond range at 1270 nm unambiguously originates from the singlet oxygen phosphorescence, which appears as a result of interaction of the nanocrystals with BSA. Appearance of the singlet oxygen generation is accompanied by the recovery in the HPPH fluorescence, as shown in the inset in Fig.5.

### ***In-Vitro* fluorescence confocal imaging of nanocrystals uptake**

To determine if HPPH nanocrystals were taken up by tumor cells, we used confocal fluorescence imaging. Though the fluorescence of nanocrystals were initially quenched, after cellular uptake the fluorescence recovered in a similar fashion as shown in case of BSA or FBS containing medium. Though, at shorter time interval, the HPPH in Tween- 80 formulation showed higher fluorescence signal, characterizing cellular uptake, after longer time of incubation (48 hrs), both showed comparable cellular uptake. This indicates that long-term cellular uptake of HPPH in nanocrystal formulations is similar to that of HPPH in Tween-80 micellar formulation. Figure 6 shows the confocal images of HPPH uptake in RIF-1 cells after 4Hrs, 24Hrs and 48 Hrs of incubation.

To elucidate whether the nanocrystal formulation need serum proteins as shuttles to deliver the HPPH into the cells, or can be directly taken up by cells, we have also incubated cells with nanocrystals without FBS in medium for 2 hrs. Cells incubated with HPPH in Tween-80 in media without FBS was used as control. As seen in Figure 7, there was significant uptake of HPPH in serum free media as well. This means that HPPH can be converted from nanocrystal to molecular form not only as a result of interaction with serum proteins, but also during interaction with cellular membrane or intracellular components. However, even if an exact mechanism of HPPH nanocrystal uptake and conversion into functional molecular form is not clearly understood, one could see that robust cellular uptake of HPPH did occur when the nanocrystal formulation was used.

### ***In Vitro* Photosensitizing Efficacy**

As shown in the Figure 8, the HPPH in the nanocrystals formulation manifested similar light dose response to the conventional Tween-80 micellar formulation, demonstrating that the efficacy of the drug *in vitro* is not affected in this surfactant-free formulation. This data is an additional confirmation of the fact that not only is the cellular uptake of HPPH as nanocrystals or in Tween-80 micelles similar, so is their efficiency of singlet oxygen generation *in vitro*.

### ***In Vivo* Photosensitizing Efficacy**

The *in vivo* efficacy of HPPH (1% Tween 80) and the HPPH nanocrystals was evaluated in C3H mice bearing RIF-1 subcutaneous tumor and the results are summarized in Figure 9. The PDT efficacy was estimated as the number of mice with minimal or no tumor regrowth after 60 days post-treatment. At day 60, 5 out of 10 mice treated with HPPH nanocrystals survived while 6 out of 10 mice survived in case of mice treated with HPPH (1% Tween 80). In the survived mice population no visual toxicity was observed. On the other hand, all the mice in the control group (received no light exposure after treatment with HPPH nanocrystals) had to be euthanized by day 8. Though there was a small difference in the survival rate (without tumor for more than 60 days) between nanocrystals and Tween80 formulation (5/10 on nanocrystal administration while 6/10 on administration of Tween80 formulation), the difference was statistically insignificant. On the other hand, between 10 and 30 days post PDT treatment, mice treated with HPPH nanocrystals formulation showed slower tumor regrowth in comparison with those treated with HPPH/Tween80 formulation. This data demonstrates that the HPPH nanocrystals formulation has comparable PDT efficacy *in vivo* to that of the conventional HPPH/Tween80 formulation, under similar treatment conditions.

### **Conclusions**

In summary, surfactant-free pure drug nanocrystals of a water-insoluble photosensitizing anticancer drug HPPH have been formulated in aqueous media. These nanocrystals are uniform in size distribution with an average diameter of 110 nm and surface charge (zeta-potential) of -40 mV. Such nanocrystals are efficiently taken up by the tumor cells *in vitro* and irradiation of such impregnated cells with light resulted in significant cell death. *In vivo* study of these drug nanocrystals also showed significant efficacy equivalent to the conventional surfactant based delivery system. These observations have illustrated the potential of using pure drug nanocrystals for PDT. This approach eliminates the need of any external agents such as surfactants or other carrier matrices for drug delivery. Further studies are underway to increase the efficacy of the nanocrystals by tuning their size, effecting long-term *in vivo* circulation and accumulation in the tumor tissue. Potentially this method of drug formulation can be applied not only for PDT drugs, but also for delivery of other therapeutic drugs including the imaging agents.

### **Acknowledgements**

This work was partially supported by grants from National Institute of Health (R01CA119358), Oishei Foundation and the Center of Excellence in Bio-informatics and Life sciences, at the University at Buffalo. Authors also acknowledge fruitful discussions with Dr. Earl J. Bergey.

### **References**

1. Konan YN, Gurny R, Allemann E. State of the art in the delivery of photosensitizers for photodynamic therapy. *Journal of Photochemistry and Photobiology B-Biology* 2002;66(2):89–106.
2. Torchilin VP. Drug targeting. *European Journal of Pharmaceutical Sciences* 2000;11:S81–S91. [PubMed: 11033430]
3. Honzak L, Sentjerc M, Swartz HM. In vivo EPR of topical delivery of a hydrophilic substance encapsulated in multilamellar liposomes applied to the skin of hairless and normal mice. *Journal of Controlled Release* 2000;66(23):221–228. [PubMed: 10742582]
4. Sobolev AS, Rozenkranz AA, Gilyazova DG. Approaches to targeted intracellular delivery of photosensitizers in order to enhance their efficacy and cell specificity. *Biofizika* 2004;49(2):351–379. [PubMed: 15129633]
5. Lukyanov AN, Torchilin VP. Micelles from lipid derivatives of water-soluble polymers as delivery systems for poorly soluble drugs. *Advanced Drug Delivery Reviews* 2004;56(9):1273–1289. [PubMed: 15109769]

6. Reddy LH. Drug delivery to tumours: recent strategies. *Journal of Pharmacy and Pharmacology* 2005;57(10):1231–1242. [PubMed: 16259751]
7. Maeda H, Greish K, Fang J. The EPR effect and polymeric drugs: A paradigm shift for cancer chemotherapy in the 21st century. *Polymer Therapeutics II: Polymers as Drugs, Conjugates and Gene Delivery Systems* 2006;193:103–121.
8. Woodburn K, Chang CK, Lee SW, Henderson B, Kessel D. Biodistribution and Pdt Efficacy of a Ketchlorin Photosensitizer as a Function of the Delivery Vehicle. *Photochemistry and Photobiology* 1994;60(2):154–159. [PubMed: 7938213]
9. Kessel D, Woodburn K. Biodistribution of Photosensitizing Agents. *International Journal of Biochemistry* 1993;25(10):1377–1383. [PubMed: 8224352]
10. Chowdhary RK, Sharif I, Chansarkar N, Dolphin D, Ratkay L, Delaney S, Meadows H. Correlation of photosensitizer delivery to lipoproteins and efficacy in tumor and arthritis mouse models; comparison of lipid-based and Pluronic P123 formulations. *Journal of Pharmacy and Pharmaceutical Sciences* 2003;6(2):198–204. [PubMed: 12935430]
11. Chowdhary RK, Shariff I, Dolphin D. Drug release characteristics of lipid based benzoporphyrin derivative. *Journal of Pharmacy and Pharmaceutical Sciences* 2003;6(1):13–19. [PubMed: 12753726]
12. Chowdhary RK, Chansarkar N, Sharif I, Hioka N, Dolphin D. Formulation of benzoporphyrin derivatives in pluronics. *Photochemistry and Photobiology* 2003;77(3):299–303. [PubMed: 12685658]
13. Dolphin D. 1993 Syntex-Award Lecture - Photomedicine and Photodynamic Therapy. *Canadian Journal of Chemistry-Revue Canadienne De Chimie* 1994;72(4):1005–1013.
14. Roy I, Ohulchanskyy TY, Pudavar HE, Bergey EJ, Oseroff AR, Morgan J, Dougherty TJ, Prasad PN. Ceramic-based nanoparticles entrapping water-insoluble photosensitizing anticancer drugs: A novel drug-carrier system for photodynamic therapy. *Journal of the American Chemical Society* 2003;125(26):7860–7865. [PubMed: 12823004]
15. Ji XH, Fu HB, Xie RM, Xiao DB, Yao JN. Perylene nanoparticles prepared by reprecipitation method. *Chinese Journal of Chemistry* 2002;20(2):123–126.
16. Ji XH, Fu HB, Cao YA, Xie RM, Zhang XT, Yao JN. Preparation and characteristics of perylene nanocrystals. *Chemical Journal of Chinese Universities-Chinese* 2001;22(8):1394–1396.
17. Fu HB, Wang YQ, Yao JN. Characterization of the optical size-dependence of pyrazolines nanocrystals. *Chemical Physics Letters* 2000;322(5):327–332.
18. Kasai H, Nalwa HS, Okada S, Oikawa H, Nakanishi H. Fabrication and spectroscopic characterization of organic nanocrystals. *Handbook of Nanostructured Materials and Nanotechnology* 2000;5:433–473.
19. Baba K, Kasai H, Okada S, Oikawa H, Nakanishi H. Fabrication of organic nanocrystals using microwave irradiation and their optical properties. *Optical Materials* 2003;21(13):591–594.
20. Prasad, PN. *Introduction to Biophotonics*. Vol. 1. Wiley-Interscience; 2003.
21. Levy JG, Obochi M. New applications in photodynamic therapy - Introduction. *Photochemistry and Photobiology* 1996;64(5):737–739. [PubMed: 8931369]
22. Fukuda H, Casas A, Batlle A. Use of ALA and ALA derivatives for optimizing ALA-based photodynamic therapy: A review of our experience. *Journal of Environmental Pathology Toxicology and Oncology* 2006;25(12):127–143.
23. Pierre MBR, Ricci E, Tedesco AC, Bentley MVLB. Oleic acid as optimizer of the skin delivery of 5-aminolevulinic acid in photodynamic therapy. *Pharmaceutical Research* 2006;23(2):360–366. [PubMed: 16341572]
24. Sharma S, Dube A, Bose B, Gupta PK. Pharmacokinetics and phototoxicity of purpurin-18 in human colon carcinoma cells using liposomes as delivery vehicles. *Cancer Chemotherapy and Pharmacology* 2006;57(4):500–506. [PubMed: 16075277]
25. Hasan, T.; Moor, ACE.; Ortel, B. *Cancer Medicine*. Vol. 5th. B.C. Decker Inc.; Hamilton: 2000. *Photodynamic Therapy of Cancer*.
26. Dougherty TJ. An update on photodynamic therapy applications. *Journal of Clinical Laser Medicine & Surgery* 2002;20(1):3–7. [PubMed: 11902352]



27. Dougherty TJ. Photodynamic Therapy (Pdt) of Malignant-Tumors. *Crc Critical Reviews in Oncology/Hematology* 1984;2(2):83–116. [PubMed: 6397270]
28. Dougherty TJ, Marcus SL. Photodynamic Therapy. *European Journal of Cancer* 1992;28A(10):1734–1742. [PubMed: 1327020]
29. MacDonald IJ, Morgan J, Bellnier DA, Paszkiewicz GM, Whitaker JE, Litchfield DJ, Dougherty TJ. Subcellular localization patterns and their relationship to photodynamic activity of pyropheophorbide-a derivatives. *Photochemistry and Photobiology* 1999;70(5):789–797. [PubMed: 10568171]
30. Peng TI, Chang CJ, Jou SB, Yang CM, Jou MJ. Photosensitizer targeting: Mitochondrion-targeted photosensitizer enhances mitochondrial reactive oxygen species and mitochondrial calcium-mediated apoptosis. *Optical and Quantum Electronics* 2005;37(1315):1377–1384.
31. Taillefer J, Jones MC, Brasseur N, Van Lier JE, Leroux JC. Preparation and characterization of pH-responsive polymeric micelles for the delivery of photosensitizing anticancer drugs. *Journal of Pharmaceutical Sciences* 2000;89(1):52–62. [PubMed: 10664538]
32. Prasad, PN. *Nanophotonics*. Vol. 1. Wiley-Interscience; 2004.
33. Pandey RK, Sumlin AB, Potter WR, Bellnier DA, Henderson BW, Constantine S, Aoudia M, Rodgers MAJ, Smith KM, Dougherty TJ. Structure and photosensitizing efficacy among alkyl ether analogues of chlorophyll-a derivatives. *Photochemistry and Photobiology* 1991;53:194–205.
34. Bellnier DA, Henderson BW, Pandey RK, Potter WR, Dougherty TJ. Murine Pharmacokinetics and Antitumor Efficacy of the Photodynamic Sensitizer 2-[1-Hexyloxyethyl]-2-Devinyl Pyropheophorbide-A. *Journal of Photochemistry and Photobiology B-Biology* 1993;20(1):55–61.
35. Pandey RK, Zheng G, Lee DA, Dougherty TJ, Smith KM. Comparative in vivo sensitizing efficacy of porphyrin and chlorin dimers joined with ester, ether, carbon-carbon or amide bonds. *Journal of Molecular Recognition* 1996;9(2):118–122. [PubMed: 8877802]
36. Lobel J, MacDonald IJ, Ciesielski MJ, Barone T, Potter WR, Pollina J, Plunkett RJ, Fenstermaker RA, Dougherty TJ. 2-[1-hexyloxyethyl]-2-devinyl pyropheophorbide-alpha (HPPH) in a nude rat glioma model: Implications for photodynamic therapy. *Lasers in Surgery and Medicine* 2001;29(5):397–405. [PubMed: 11891727]
37. Anderson TM, Dougherty TJ, Tan DF, Sumlin A, Schlossin JM, Kanter PM. Photodynamic therapy for sarcoma pulmonary metastases: A preclinical toxicity study. *Anticancer Research* 2003;23(5A):3713–3718. [PubMed: 14666668]
38. Bellnier DA, Greco WR, Nava H, Loewen GM, Oseroff AR, Dougherty TJ. Mild skin photosensitivity in cancer patients following injection of Photochlor (2-[1-hexyloxyethyl]-2-devinyl pyropheophorbide-a; HPPH) for photodynamic therapy. *Cancer Chemotherapy and Pharmacology* 2006;57(1):40–45. [PubMed: 16001178]
39. Kasai H, Nalwa HS, Oikawa H, Okada S, Matsuda H, Minami N, Kakuta A, Ono K, Mukoh A, Nakanishi H. A novel preparation method of organic microcrystals. *Japanese Journal of Applied Physics, Part 2: Letters* 1992;31(8A):L1132–L1134.
40. Oikawa H, Mitsui T, Onodera T, Kasai H, Nakanishi H, Sekiguchi T. Crystal size dependence of fluorescence spectra from perylene nanocrystals evaluated by scanning near-field optical microspectroscopy. *Japanese Journal of Applied Physics Part 2-Letters* 2003;42(2A):L111–L113.
41. Frederiksen PK, Jorgensen M, Ogilby PR. Two-photon photosensitized production of singlet oxygen. *Journal of the American Chemical Society* 2001;123(6):1215–1221. [PubMed: 11456676]
42. Ohulchanskyy TY, Donnelly DJ, Detty MR, Prasad PN. Heteroatom substitution induced changes in excited-state photophysics and singlet oxygen generation in chalcogenoxanthylum dyes: Effect of sulfur and selenium substitutions. *Journal of Physical Chemistry B* 2004;108(25):8668–8672.
43. Dedic R, Molnar A, Korinek M, Svoboda A, Psencik J, Hala J. Spectroscopic study of singlet oxygen photogeneration in meso-tetra-sulphonatophenyl-porphin. *Journal of Luminescence* 2004;108(14):117–119.
44. Korinek M, Dedic R, Svoboda A, Hala J. Luminescence study of singlet oxygen production by meso-tetraphenylporphine. *Journal of Fluorescence* 2004;14(1):71–74. [PubMed: 15622863]
45. Salokhiddinov KI, Byteva IM, Dzagezov BM. Lifetime of singlet oxygen luminescence in solution under pulsed laser excitation. *Opt Spectrosc (USSR)* 1979;47:881–886.

46. Losev AP, Byteva IM, Gurinovich GP. Singlet Oxygen Luminescence Quantum Yields in Organic-Solvents and Water. *Chemical Physics Letters* 1988;143(2):127–129.
47. Zenkevich E, Sagun E, Knyukshto V, Shulga A, Mironov A, Efremova O, Bonnett R, Songca SP, Kassem M. Photophysical and photochemical properties of potential porphyrin and chlorin photosensitizers for PDT. *Journal of Photochemistry and Photobiology B-Biology* 1996;33(2):171–180.
48. Li G, Graham A, Chen Y, Dobhal MP, Morgan J, Zheng G, Kozyrev A, Oseroff A, Dougherty TJ, Pandey RK. Synthesis, Comparative Photosensitizing Efficacy, Human Serum Albumin (Site II) Binding Ability, and Intracellular Localization Characteristics of Novel Benzobacteriochlorins Derived from *vic*-Dihydroxybacteriochlorins. *Journal of Medicinal Chemistry* 2003;46(25):5349–5359. [PubMed: 14640543]
49. Bellnier DA, Greco WR, Loewen GM, Nava H, Oseroff AR, Pandey RK, Tsuchida T, Dougherty TJ. Population Pharmacokinetics of the Photodynamic Therapy Agent 2-[1-Hexyloxyethyl]-2-devinyl Pyropheophorbide-a in Cancer Patients. *Cancer Res* 2003;63(8):1806–1813. [PubMed: 12702566]
50. Yuzhakov VI. Aggregation of Dye Molecules and Its Effect on Spectral-Luminescent Properties of Solutions. *Uspekhi Khimii* 1992;61(6):1114–1141.

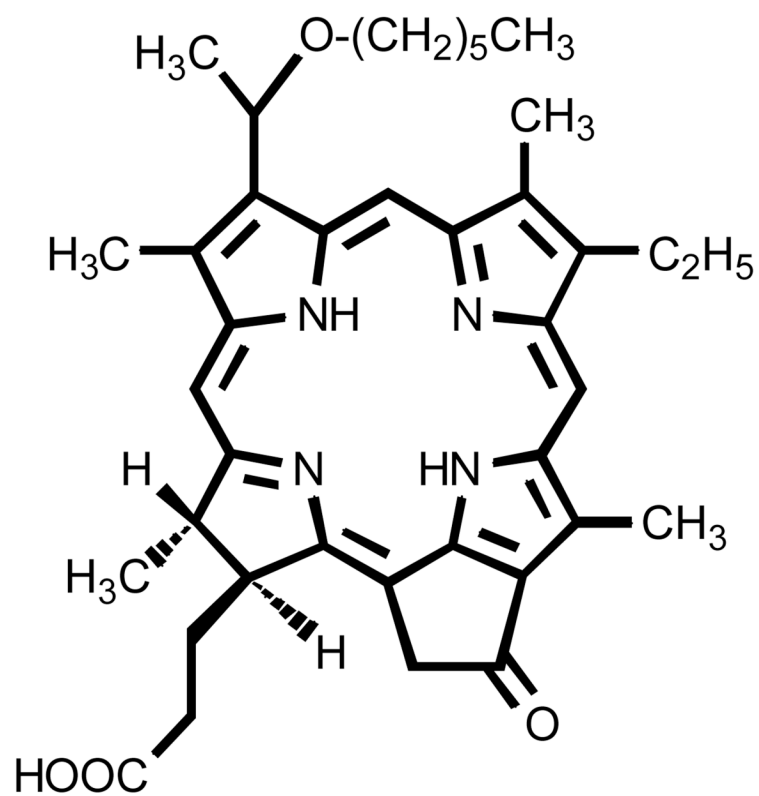


**Figure 1.**  
Structure of the HPPH

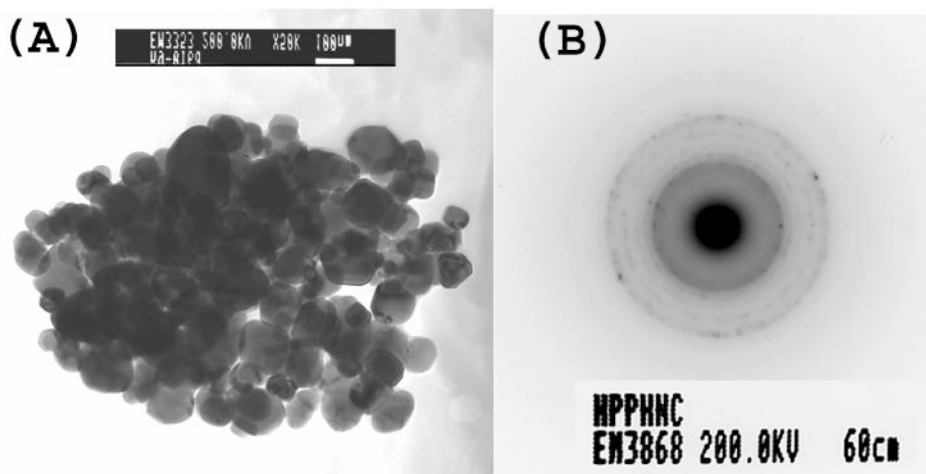


**Figure 2.**  
(A) TEM picture of HPPH nanocrystals (B) Electron diffraction from HPPH nanocrystals

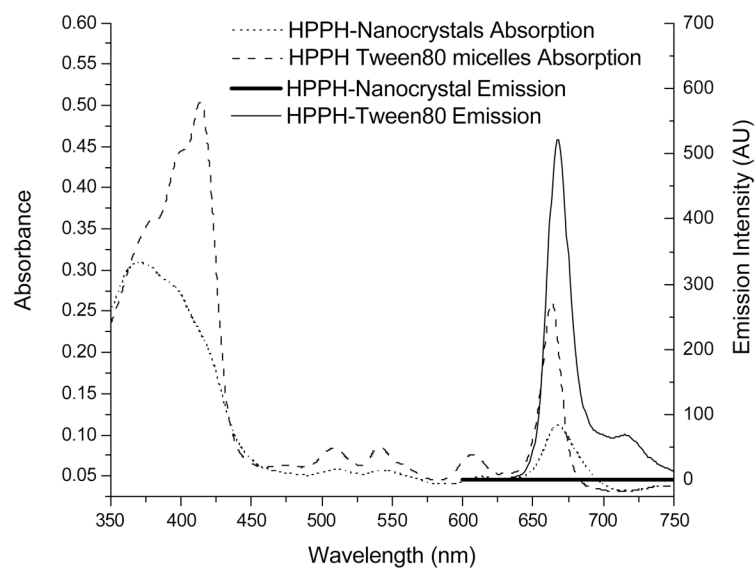


**Figure 3.** Absorption and emission spectra of HPPH nanocrystals (4 μM) in comparison with Tween-80 micellar formulation at the same molar concentration in water.



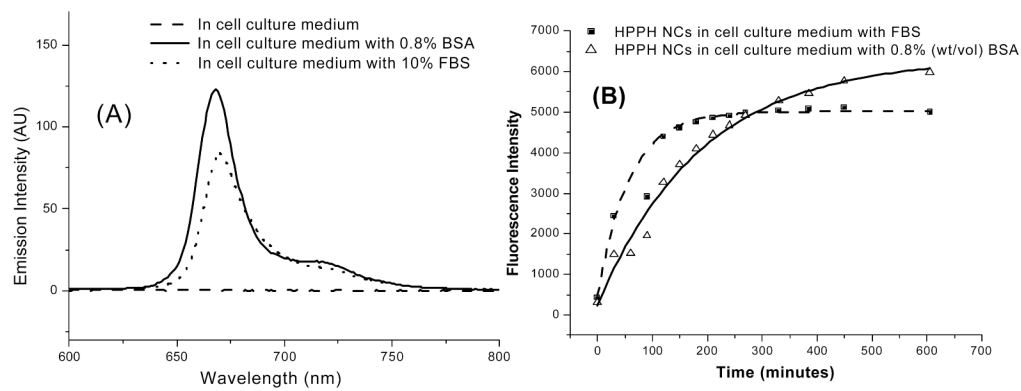


**Figure 4.**

(A) Fluorescence signal from HPPH nanocrystals ( $4 \mu\text{M}$ ) in pure cell culture medium ( $\text{MEM}\alpha$ ) and  $\text{MEM}\alpha$  with added FBS or BSA after 6 hrs of incubation at room temperature; (B) Time-dependent fluorescence signal recovery from HPPH nanocrystals ( $4 \mu\text{M}$ ) in pure  $\text{MEM}\alpha$  and  $\text{MEM}\alpha$  with added FBS (10% v/v) or BSA (0.8% w/v).

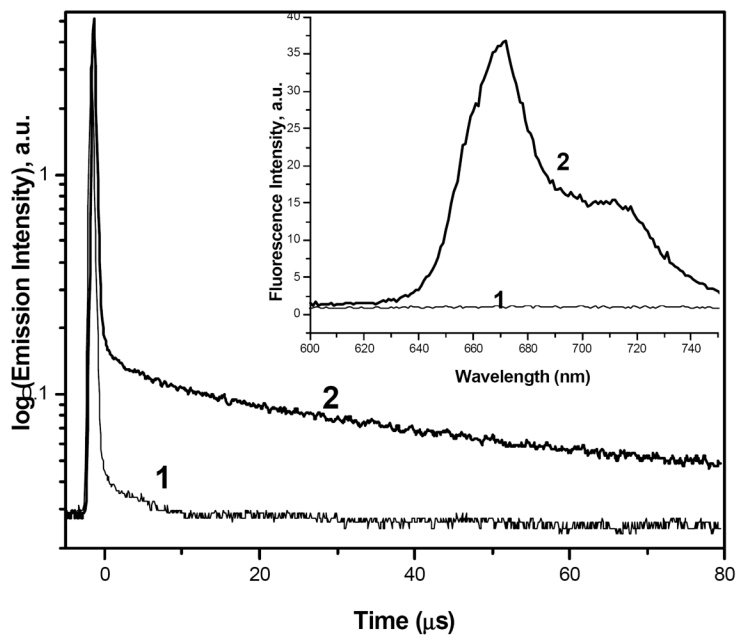


**Figure 5.** Singlet oxygen phosphorescence decay monitored at 1270nm (1) HPPH nanocrystals in MEM $\alpha$  cell culture media and (2) HPPH nanocrystals incubated with MEM $\alpha$  and 0.8% BSA for 24 Hrs. The inset figure shows the corresponding fluorescence recovery. Concentration of HPPH was 45 $\mu$ M.

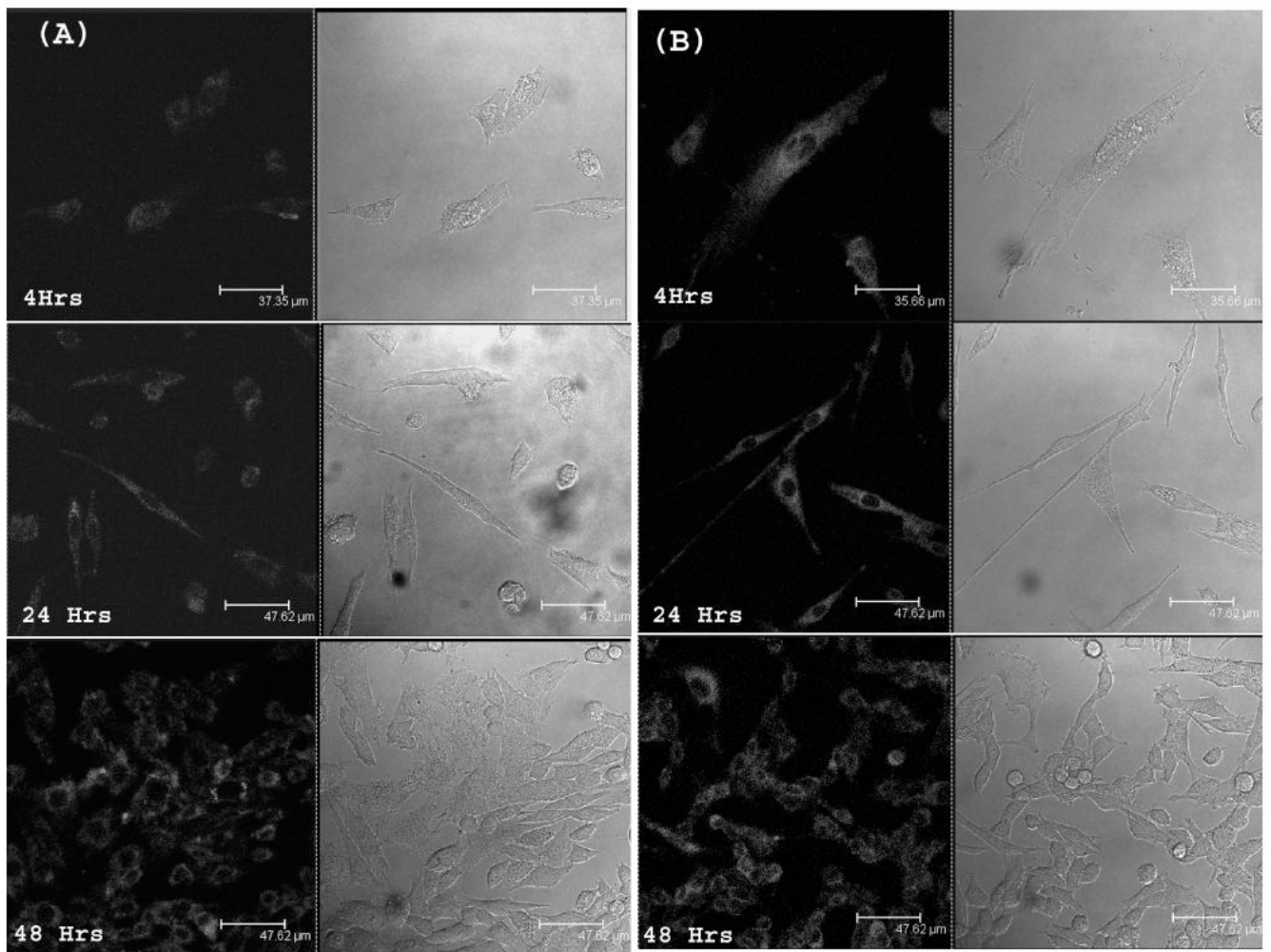


**Figure 6.** Confocal fluorescence images of RIF-1 cells imaged after 4 hrs, 24hrs and 48 hrs of treatment with HPPH nanocrystals (A) and tween-80 micellar formulation (B). Drug concentration was maintained at 0.5  $\mu\text{M}$ . Cells were incubated in medium containing 10% of FBS.

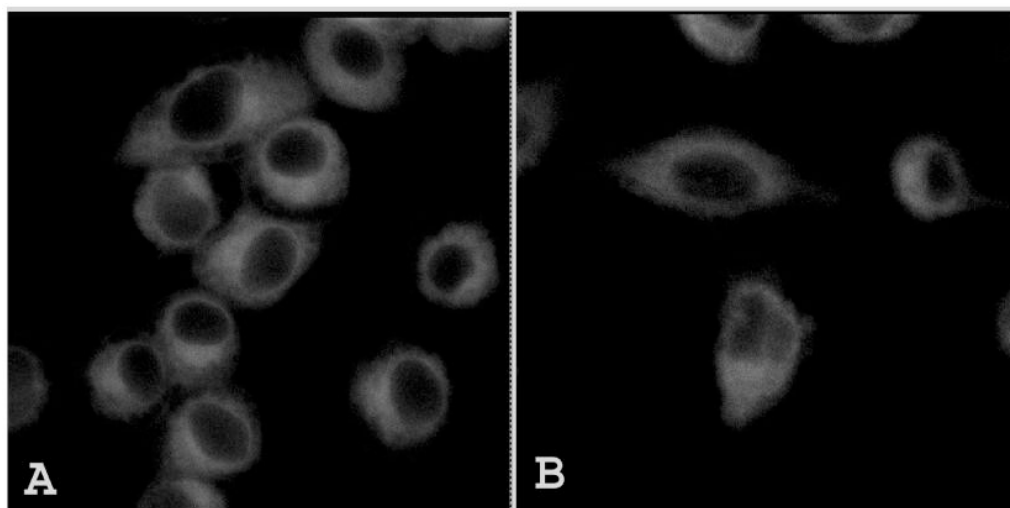


**Figure 7.** Confocal fluorescence images of RIF-1 cells incubated with (A) Tween 80 micellar formulation and (B) HPPH nanocrystals, imaged after 2 hrs of incubation in serum free media. Excitation wavelength used was 405nm.

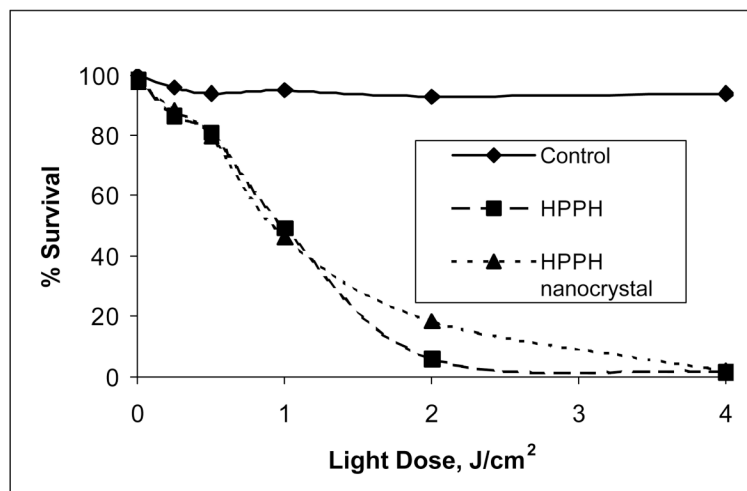


**Figure 8.** Comparative *in vitro* photosensitizing efficacy of HPPH formulated in 1% Tween 80/5% dextrose and HPPH nanocrystals/water in RIF-1 cells at equimolar concentrations ( $0.5\mu\text{M}$ ). Control: Cells were exposed to light without photosensitizer.



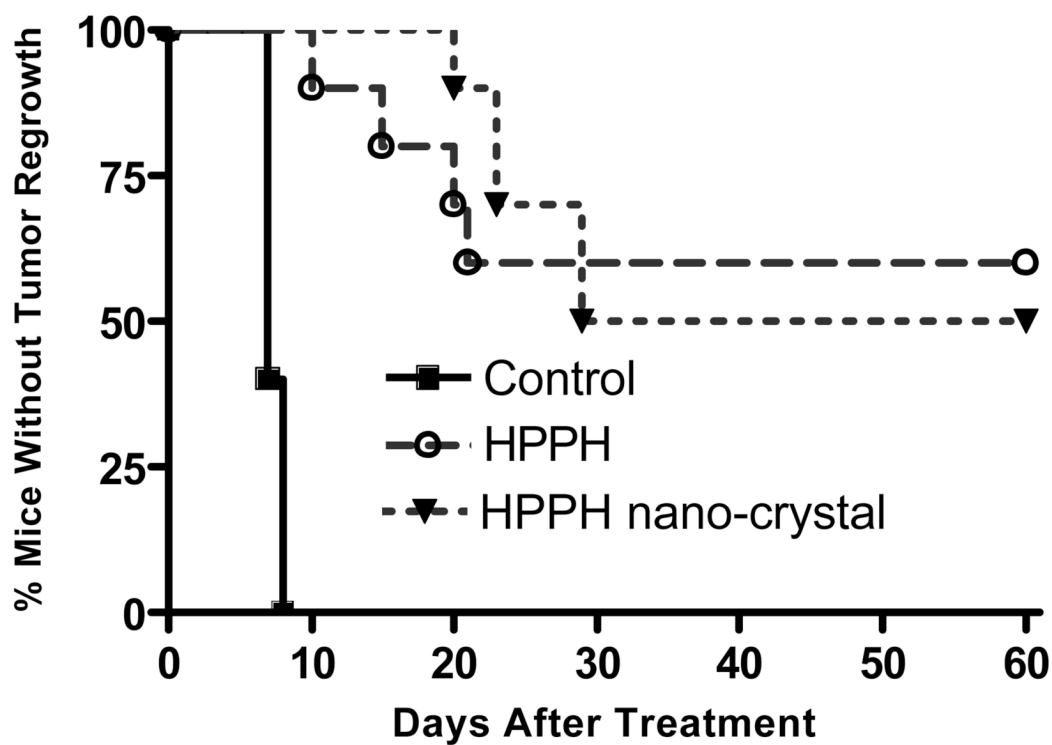


**Figure 9.** Comparison of *in vivo* photosensitizing efficacy of HPPH nanocrystals and Tween 80 micellar formulation in C3H mice (10 mice/group) bearing RIF-1 tumors. The tumors were exposed to a laser light (665 nm, 135 J/cm<sup>2</sup>) at 24 h after injection. Drug dose: 0.4  $\mu$  mole/kg. Control: The mice were injected with HPPH nanocrystals, without any light exposure.